Glacier Volume Changes Using ASTER Satellite Stereo and ICESat GLAS Laser Altimetry. A Test Study on Edgeøya, Eastern Svalbard

Andreas Kääb, *Member, IEEE*

***Abstract*—Currently, one of the major methodological gaps in the observation of glaciers from space is the measurement of volume changes of mountain glaciers and ice caps. In this paper, we present a case study of comparing a digital elevation model derived from Advanced Spaceborne Thermal Emission and Reflection Radiometer (ASTER) satellite optical stereo, elevation data derived from Ice, Cloud, and land Elevation Satellite Geoscience Laser Altimeter System (GLAS) laser altimetry, and contour lines from a topographic map from the 1970s. For two ice caps in Eastern Svalbard, Kvalpyntfonna and Digerfonna, we obtain an overall elevation change of -0.55 or -0.61 m/year between 1970 and 2002 (ASTER) or GLAS (2006), respectively. From comparison of different methods and from different quality checks, we estimate the error of this numbers to be on the order of 5%. This paper demonstrates that and on how long-term glacier volume changes can be observed from space over a large number of ice caps and glaciers.**

***Index Terms*—Advanced Spaceborne Thermal Emission and Reflection Radiometer (ASTER) stereo, glacier volume change, Ice, Cloud, and land Elevation Satellite (ICESat) Geoscience Laser Altimeter System (GLAS) laser altimetry, Svalbard.**

I. Introduction

SPACEBORNE techniques are the only method for sustainable global-scale monitoring of glaciers. Whereas spaceborne methods have been developed and successfully applied for detecting glacier area changes and glacier movement, the major current gap in glacier monitoring from space lies in the measurement of glacier volume changes. Radar altimetry (ERS and ENVISAT radar altimeters) and synthetic-aperture-radar (SAR) interferometry are, in principle, applicable for this purpose but severely complicated or even excluded from use over the rough topography and small scale of mountain glaciers and small ice caps. Except for tandem missions, repeat-pass SAR interferometry for generation of digital terrain models (DTMs) over glaciers commonly suffers from phase decorrelation due to ice melt, snow accumulation, ice flow, etc. The single-pass synthetic aperture radar (SAR) interferometry Shuttle Radar Topography Mission (SRTM) managed by NASA provides a highly valuable data set of glacier elevation in the year 2000; however, only for latitudes between 54° S and 60° N [1]–[3]. Consequently, SRTM data are not available for, e.g., Svalbard. Satellite (optical) stereo is, therefore, considered to be one future key technology for measuring glacier volume changes from space, applied alone or complementing altimetry and SAR interferometry methods. Due to the fast temporal changes of ground and illumination conditions in glacial and mountain environments such as snow accumulation, snow melt, topographic shadowing, etc., along-track stereo is often preferable over cross-track stereo.

So far, only a few studies have applied satellite optical stereo to estimate changes in glacier elevation or glacier volume, for the most part, using SPOT [4]–[6] and Advanced Spaceborne Thermal Emission and Reflection Radiometer (ASTER) [7]–[11] data. Although optical-stereo sensors of higher spatial resolution than ASTER such as SPOT5, ALOS PRISM, Ikonos, or Quickbird are meanwhile available, the advantage of the Japan-built sensor ASTER onboard the NASA Terra spacecraft is the large global data set acquired since early 2000. This significantly increases the probability of finding suitable data in the archives and even possibly of generating time series. ASTER's visible and near-infrared (VNIR) sensors include a near-infrared (NIR) nadir band (3N) and an along-track back-looking stereo band with about 30° off-nadir viewing angle (3B) of the same wavelength range, both having a medium spatial resolution of 15 m [12], [13].

Besides satellite stereo, spaceborne laser altimetry is another promising technology for monitoring glacier elevation and volume changes. Indeed, data of the Geoscience Laser Altimeter System (GLAS) onboard the NASA Ice, Cloud, and land Elevation Satellite (ICESat) [14] have been successfully used to detect vertical changes of glaciers [3], [6], [15]–[17]. GLAS footprints have a diameter of approximately 70 m and an along-track ground spacing of about 170 m. The ground coordinates of GLAS-footprint centers are known with an accuracy of a few meters for recent releases.

Here, we produce elevation data over two ice caps in eastern Svalbard from an ASTER scene of summer 2002 and compare the data to elevation data from the ICESat GLAS laser altimeter (release 428) and to contour lines from a topographic map from the 1970s in order to derive changes in glacier thickness and volume. The purpose of this paper is to investigate data, methods, and their accuracies for deriving glacier volume changes on regional scales using satellite stereo, satellite laser altimetry, and topographic maps.

Our test sites are the Digerfonna and Kvalpyntfonna ice caps to the southwest of Edgeøya, eastern Svalbard (Figs. 1 and 2)

Manuscript received October 1, 2007; revised January 28, 2008 and April 5, 2008. Current version published October 1, 2008. This work was supported in part by the Norwegian International Polar Year project GLACIODYN and by the European Space Agency DUE GlobGlacier project.

The author is with the Department of Geosciences, University of Oslo, 0316 Oslo, Norway (e-mail: kaeaeb@geo.uio.no).

Color versions of one or more of the figures in this paper are available online at http://ieeexplore.ieee.org.

Digital Object Identifier 10.1109/TGRS.2008.2000627

0196-2892/$25.00 © 2008 IEEE

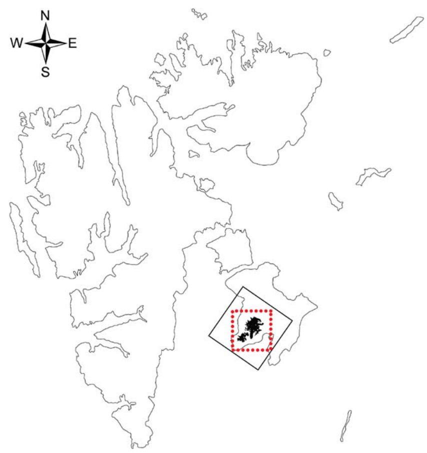

Fig. 1. Svalbard, location of the ASTER scene used (black rectangle) and the section shown in Fig. 2 (dotted inner rectangle). ASTER scene size is approximately 60 km × 60 km.

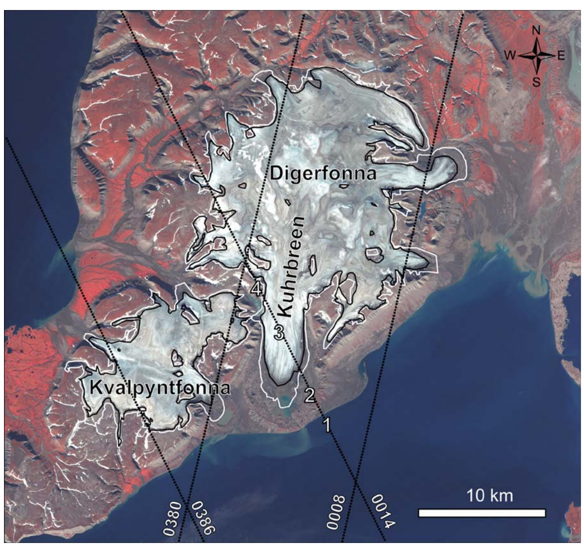

Fig. 2. Section of the ASTER scene of 13 August 2002. The white glacier outlines are from 1970/71, the black glacier outlines from the ASTER scene. The dotted lines and numbers along them indicate the ICESat tracks available (0008, 0014, 0380, 0386). Numbers 1–4 on the ICESat track 0014 indicate the position of example waveforms (Fig. 4).

[18]. The glaciers on the Svalbard archipelago are believed to currently provide a significant volume contribution to sea-level rise [19]. Particularly little is known about glacier changes in eastern Svalbard.

II. Data and Methods

A. Topographic Maps

As reference data set, we use topographic maps from the 1 : 100 000-scale series by the Norwegian Polar Institute. In the test region, this topographic map was photogrammetrically compiled based on 1 : 50 000-scale airphotos taken in midsummer of 1970 and 1971 (the original airphotos are not available to us). The size and number of snow fields on the map are comparable to the snowfields found on the ASTER satellite image, which leads us to conclude that the snow conditions in midsummers 1970/1971 and 2002 were similar, and the glacier margins thus free of snow for most sections in 1970 and 1971, as they are also in the ASTER data (Fig. 2). The topographic map includes glacier outlines and contour lines, the latter with 50-m vertical spacing, in some flat coastal areas with 25-m vertical spacing. According to standard empirical values for photogrammetric height measurement (Koppe's formula), the vertical accuracy of the contour lines could be up to ±3–4 m for areas with sufficient radiometric contrast in the images. For selected nonglaciated zones of the study area, we compare contour-line elevations to ICESat GLAS elevations and obtain an average root mean-square (rms) deviation of ±12 m (see Section III-B).

The contour lines and glacier outlines are digitized from the scanned and georeferenced topographic maps. This is done for the glaciated areas and a buffer of several kilometers around the two main ice caps (see Fig. 5).

B. Photogrammetric DTM From ASTER

For the generation of a more recent DTM over the test site, we use an ASTER scene of August 13, 2002 (Fig. 2). Out of the roughly 50 ASTER scenes available for the two ice caps or large parts of it, about 20% are cloud free and with little snow remains outside the glaciated areas. The scene chosen here is, however, clearly the best in terms of geographic coverage and radiometric contrast and snow conditions on the glaciers. Using the 3-D physical sensor model within the PCI Geomatica software [12], the orientation of the data is determined using ground control points (GCPs) taken from the 1 : 100 000-scale map. ICESat GLAS elevation data were not used as height control points (see Section III-B). The rms accuracy of the sensor model solution using the GCPs, the so-called bundle block adjustment, i.e., the transformation from image to ground space, is ±2.5 pixels (i.e., ±37 m).

From the ASTER 3N and 3B stereo data, DTMs with 30-, 60-, and 120-m resolutions are computed (for details on the procedures, see, e.g., [8], [10], and [13]). The different resolution levels of this DTM pyramid are compared to each other to detect large DTM errors [8]. No gross vertical deviations between the DTMs from different image-pyramid levels were found over the glacier areas and around them. In fact, the correlation values from parallax matching show high values for almost all DTM points on the glacier areas (Fig. 3) due to the strong melt-out of the ice and corresponding high radiometric contrast (Fig. 2). For 98.5% of the DTM points over ice, that are about 60 000 for 60-m DTM resolution, the correlation value is over 0.8. The mean correlation coefficient over ice is 0.92 and 0.87 outside.

To further check the quality of the final DTM (60-m grid), orthoimages are produced both from the ASTER 3N and the 3B data. Comparing orthoimages that are based on image data taken from different directions allows us rapid visual identification of vertical DTM errors, since such vertical errors result in horizontal shifts between corresponding points in the two orthoimages [8].

All three steps of DTM quality check, resolution pyramid, matching correlation coefficients, and overlay of orthoimages computed from different viewing angles, allow us to roughly estimate the DTM quality in the absence of independent

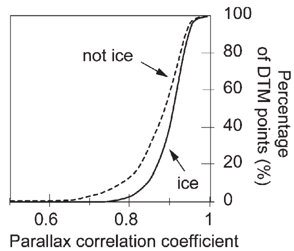

Fig. 3. Cumulative histogram of correlation coefficients from ASTER height–parallax matching for (solid line) glacier and (dashed line) land areas outside the glaciers.

reference data. Here, we estimate the rms error of an individual elevation point in the raster DTM to be on the order of ±15-m rms for areas with good radiometric contrast [8], [12].

C. ICESat GLAS Laser Altimetry Data

As a third data set, we use ICESat GLAS data, release 428, available from the National Snow and Ice Data Center (NSIDC) [20]. Due to the mountain topography in the study area, we use the GLA14 product instead of the GLA06 product that is usually applied for ice sheets [15], [21]. In the GLA06 product, ground elevation is determined from the position of the centroid of the maximum peak of no more than two Gaussian fits of the return signal (ice-sheet parameterization). In the GLA14 product, a maximum of six Gaussians are fitted to the return signal in order to account for a more complex elevation structure within the footprint (land parameterization) [21]. Since the decision of preferring GLA14 over GLA06 is certainly open to discussion, we also compare both products for the study area. The average elevation difference between both products over the glaciated area is 0.14 m ±0.4 m rms and 0.01 m ±0.8 m rms outside. The standard error of this means is on the order of ±0.1 m, with maximum differences up to about ±6 m. The mean difference between both products is therefore hardly significant for the study area.

The data are transformed to the WGS84 system. Out of all GLAS data available for the test site for the autumns of 2003, 2004, 2005, and 2006, we select for each year the first track with a significant number of elevation data over the study area in the data granule in order to reduce elevation effects from seasonally varying snow thickness. The GLAS data are also checked for cloud cover using the ASTER DTM. GLAS elevations are not accepted, if the difference is larger than 200 m. From the finally used tracks, 32 footprints are removed that way. In addition, we check the full waveform for a number of locations and dates (Fig. 4). About 13% of the GLAS footprints showed detector saturation with a mean saturation range correction of 0.8 m. Any effects of, for example, topography on the GLAS footprint shapes were not taken into account, assuming that they result in a random vertical error which then has little effect on the final mean glacier-elevation change aimed at in this paper. The data finally used were acquired on October 22, 2003 (tracks 0008 and 0014; laser period 2A), November 16, 2003 (0380 and 0386; 2A), October 9 and 10, 2004 (0008 and 0014; 3A), November 3 and 4, 2004 (0380 and 0386; 3A), October 27, 2005 (0008 and 0014; 3D), October 30 and 31, 2006 (0008 and 0014; 3G),

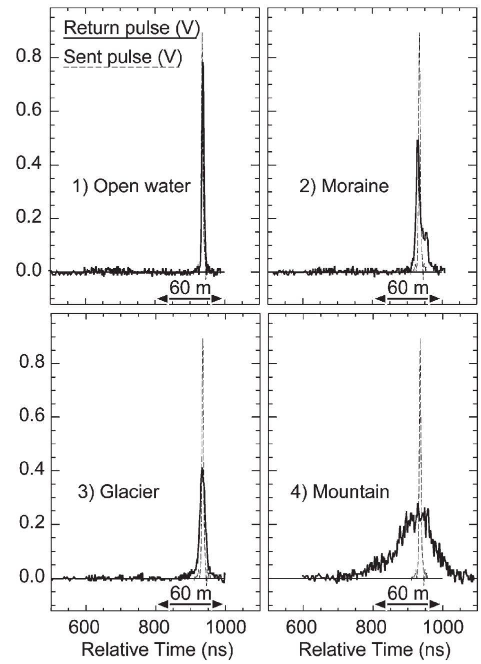

Fig. 4. Selected ICESat GLAS waveforms of laser period 3G for typical surfaces of this paper (for locations, see Fig. 2).

and November 24 and 25, 2006 (0380 and 0386; 3G). Four different nominal ICESat ground tracks with approximately 210 footprints intersect with the two ice caps investigated in this paper (Fig. 2).

D. Area Changes

The ice-cap areas for 1970/1971 are calculated from the digitized outlines. For 2002, the ice-cap outlines are manually digitized from an ASTER VNIR false-color composite, which is for that purpose orthorectified using the ASTER DTM. Automatic delineation of the outlines from the satellite image is also possible [22] but would have been more time consuming for such small areas. Table I shows the obtained glacier areas and area changes.

E. Calculation of Elevation Differences

For differentiating the 1970/1971 contour lines and the 2002 ASTER DTM, the vertices of the contour lines, that are the node points between the individual line segments, are intersected with the ASTER DTM so that each vertex is assigned both a 1970/1971 and a 2002 elevation. This procedure avoids interpolation artifacts caused by the sparsely distributed contour lines and relies instead on the original data. We also interpolate a 1970/1971 DTM from the contour lines for difference calculation.

As a final step toward calculating glacier elevation differences, the 1970/1971 contour lines from outside the ice caps and at rock outcrops within them are compared to the ASTER-derived DTM. There is a slight dependence between elevation difference and elevation of +4 m per 100-m elevation. This distortion of the stereo model with elevation could be due to the unfavorable distribution of GCPs used for the ASTER data orientation. Large parts of the scene are ocean

TABLE I
ICE-CAP AREAS, AREA CHANGES, AND MEAN THICKNESS CHANGES BETWEEN 1970/1971 AND 2002

	Digerfonna	Kvalpyntfonna	Total
1970/71	263 km^2	84 km^2	347 km^2
2002	225 km^2	67 km^2	292 km^2
Area change	-38 km^2 (-17 %)	-17 km^2 (-25%)	-55 km^2 (-19%)
Thickness change 1970/71 to 2002 from ASTER	-20.3 m (-0.65 m/yr)	-9.2 m (-0.30 m/yr)	-17.5 m (-0.55 m/yr)
Thickness change 1970/71 to 2006 from ICESat	—	—	- 21.8 m (-0.61 m/yr)

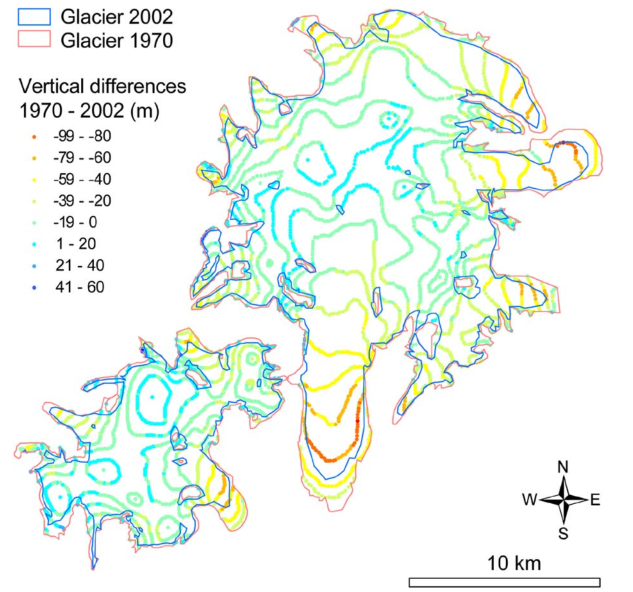

Fig. 5. Elevation differences between map contour time of 1970/1971 and the 2002 ASTER DTM for the glacier areas.

with no GCPs available, whereas most of the high-elevation GCPs are difficult to identify in the satellite data due to the typical plateau topography on Edgeøya without distinct peaks (Fig. 2). The distortion effect is accounted for as an overall linear correction applied to elevation differences between the ASTER DTM and the contour lines. Fits of higher polynomial order do not reveal significantly different figures. The residuals from the regressions show an rms error for the ASTER DTM points outside the ice caps of about ± 20 m after correction.

The steps explained so far give 1970/1971 elevations, 2002 elevations, and the respective differences at each contour-line vertex (Fig. 5). In order to compare the GLAS data to the ASTER DTM, the ASTER DTM is intersected at the center-point location of each GLAS footprint, resulting in elevations for 2002 and 2003, 2004, 2005, or 2006 and corresponding elevation differences at each GLAS footprint over the two ice caps.

To compare the GLAS data to the 1970/1971 contour lines, a buffer of 150-m width is constructed around the contour lines and their elevation assigned to the GLAS footprints within the corresponding buffers. The size of this buffer is certainly open to discussion. In the case of our test site, the maximal offset of 75 m of a selected GLAS footprint center from a contour line leads to an average elevation error of about ± 3 m, resulting from an average surface slope between 2° and 3° on the ice caps. Because this error is randomly distributed, it should have little effect on the mean elevation differences and volume changes, which are the main emphases of this paper. Similarly, we assume that elevation errors due to pointing uncertainty and due to the variable GLAS footprint size and ellipticity over the different laser periods and overpasses are randomly distributed or have little effect in relation to the large elevation changes investigated because of the low slope and smooth topography on the two ice caps studied. About 70 of the 210 nominal GLAS footprints covering the ice caps lie within the above contour-line buffers. From all GLAS acquisition dates used for this paper, a total of approximately 180 footprints with accepted quality (no clouds) are located within the contour-line buffers and are used for calculating elevation differences between 1970/1971 and the 2003–2006 GLAS data.

III. RESULTS

We perform the following procedures to assess glacier volume changes over Digerfonna and Kvalpyntfonna:

1) interpolate elevation differences that are calculated between the map contour lines and the ASTER-derived DTM;
2) interpolate a DTM from the contour lines and subtract it from the ASTER-derived DTM;
3) multiply the average elevation difference per elevation level between contour lines and the ASTER-derived DTM with the total glacier area in each elevation interval (hypsography method);
4) estimate an analytical relation between the elevation changes from 1) and glacier-surface elevation and integrate this average relation over the entire glaciated area;
5) compare GLAS footprint elevations to the ASTER-derived DTM;
6) compare GLAS footprint elevations to the map contour lines;
7) analogously to 3), using GLAS instead of ASTER elevations;
8) analogously to 4), estimate an analytical relation between the elevation differences from 6) and surface elevation and integrate this average relation.

A. ASTER DTM Versus Map Contour Lines

Fig. 5 shows the raw differences between the 2002 ASTER DTM and the vertices of the 1970/1971 contour lines.

For method 1), raw elevation differences at contour-line vertices are interpolated using spline, kriging, and inverse-distance-weighting algorithms. The results of these three interpolation techniques show little difference, mainly due to the low spatial gradients and the lack of gross outliers in the elevation differences, which could severely impact interpolation and the corresponding volume-change estimates. The average of all three interpolations is shown in Fig. 6. All three

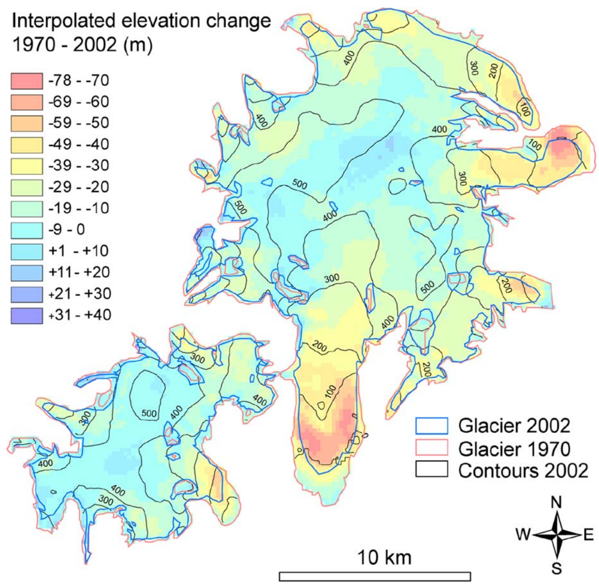

Fig. 6. Elevation differences interpolated from Fig. 5.

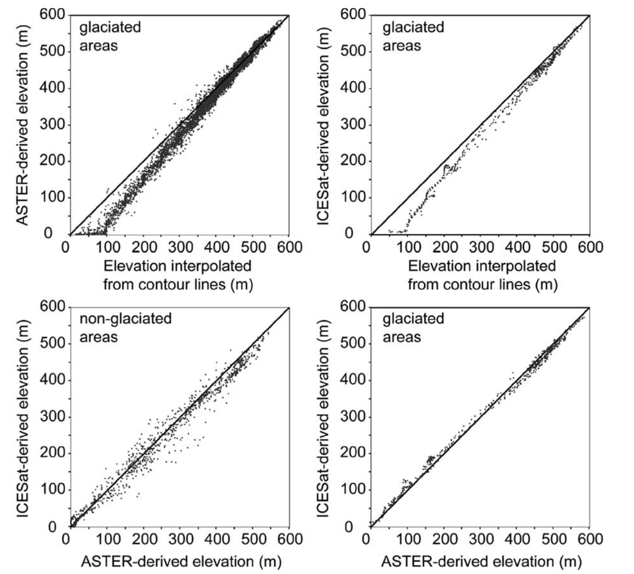

Fig. 7. Scatter plots of elevations from GLAS, ASTER, and map contour lines against each other.

interpolations give an average elevation change of −18.2 m between 1970/1971 and 2002 (−0.59 m/year).

In method 2), we interpolate a 1970/1971 DTM from the contour lines and subtract it from the ASTER DTM. Compared to method 1), method 2) introduces artifacts from interpolating a 1970/1971 DTM from the scarcely distributed contour lines but does, on the other hand, use all ASTER-derived elevations (Fig. 7). The resulting mean elevation difference from method 2) is −17.2 m (−0.55 m/year). The mean difference between the elevation differences from methods 1) and 2) is 1 ± 12 m rms. The latter rms error indicates, among others, the size of interpolation artifacts through method 2).

In method 3), we calculate the average elevation difference between contour-line vertices and the ASTER DTM for each 50-m elevation level and multiply these numbers with the total glacier area at this elevation level (hypsography in Fig. 8). For both ice caps together, we obtain −17.5 m between 1970/1971 and 2002 (−0.56 m/year).

In method 4), for computing the overall elevation change, we plot raw elevation differences (corrected for the elevation-dependent bias; Section II-E) against elevation in order to compute the average elevation change as a function of elevation. Topographic parameters other than elevation could also be taken as independent variables for such relation, but ice thickness changes are, in most cases, strongly linked to elevation, for glaciological and meteorological reasons (e.g., [1]). Fig. 8 shows the averages and the rms errors for individual elevation zones of Kuhrbreen, the largest glacier of the Digerfonna ice cap, and the sixth-order polynomial regressions for Kuhrbreen, Digerfonna, Kvalpyntfonna, and both ice caps together. The order of the polynomial regressions is iteratively chosen by increasing it until the improvement of the rms to a higher order is smaller than ±0.05 m. It is important to note that the rms of elevation differences as given for each 50-m elevation zone is not only a result of a) vertical errors in the ASTER DTM but also of b) horizontal errors of the contour-line location and c) natural variations of thickness change at a certain glacier elevation. These errors will combine as root sum square (RSS).

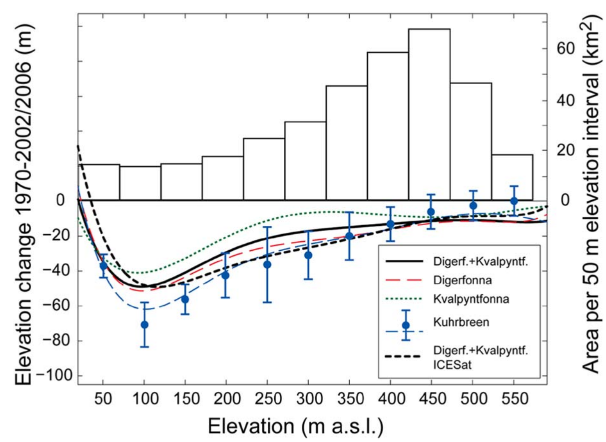

Fig. 8. (Upper part) Hypsography of both ice caps. (Lower part) Glacier elevation changes as an interpolated polynomial function of surface elevation. For both ice caps together, also the relation between the contour lines and 2006 ICESat data is given. The average values and rms for each 50-m-elevation level are exemplified for Kuhrbreen.

The rms errors of the polynomial fits range from ±12 m for Kuhrbreen, an individual outlet glacier, to ±15 m for both ice caps together.

From the mean relation between elevation change and elevation, we obtain by integration over the entire ice caps an average elevation change of −16.9 m between 1970/1971 and 2002 for both ice caps together (−0.54 m/year).

B. ICESat GLAS Versus Map Contours and ASTER DTM

About 930 accepted GLAS footprints of the ICESat data used here overlap with the ASTER DTM outside the ice caps. ASTER DTM elevations were intersected for each GLAS footprint individually and GLAS repeat tracks not intercompared, so that horizontal offsets between the repeat tracks have no direct impact on the elevation differences computed [3]. The average difference between the ICESat

TABLE II
SUMMARY OF VERTICAL DIFFERENCES BETWEEN THE DIFFERENT ELEVATION DATA SETS USED

	Non-glaciated land areas (Mean ± RMS)	Glaciated areas; at contour line positions (Mean ± RMS)
2002 ASTER DTM – 2003-2006 ICESat GLAS	-1.4 ±24 m	-3.9 ±10 m (-3.8 ±12 m complete data set)
2002 ASTER DTM – 1970/71 contour lines	-3.1 ±21 m	-16.5 ±21 m
2003-2006 ICESat GLAS – 1970/71 contour lines	+1.8 ±12 m	-20.4 ±18 m

GLAS elevations and the ASTER DTM is -1.4 ± 24-m rms (-1.3 m with the saturation correction applied) with a marginally significant average linear trend of about -3 m per 100-m elevation (Table II, cf. Fig. 7). The good vertical agreement between the ASTER DTM and ICESat-derived elevations suggests that use of GLAS footprints as additional height or 3-D control points during the orientation of the ASTER stereo model is not necessary in this paper [17], [23].

The difference between the 2002 Terra ASTER DTM and the combined ICESat GLAS elevation data over the ice caps is calculated for the autumns 2003, 2004, and 2006 [method 5)]. The 2005 ICESat track is excluded, because it intersects only a few outlet glaciers of Digerfonna and would thus bias the calculation of glacier volume changes. At the remaining $\sim$400 footprint locations within the ice-cap areas, the mean difference between ICESat- and ASTER-derived elevations is -3.8 ± 12.0-m rms (-3.7 m with saturation correction applied; 2003: -0.6 m, -0.5 m/year; 2004: -1.5 m, -0.7 m/year; 2006: -5.7 m, -1.3 m/year).

We manually select approximately 100 GLAS footprints which overlap within 35 m with 1970/1971 contour lines outside the glaciated area. In order to select topographic conditions similar to the ice caps, we thereby avoid steep flanks of the plateau-type mountains and potentially changed dead-ice zones around the glacier tongues. The result is a vertical offset between GLAS elevations and 1970/1971 contour lines of 1.8 ± 12-m rms (1.9 m with saturation correction applied; Table II). This rms error of ± 12 m is mainly a combined effect (RSS) of the contour-line accuracy, GLAS elevation accuracy, and the horizontal offset between the contour-line position and the GLAS footprint center. The vertical accuracy of the contour lines in the selected zones is therefore certainly better than ± 12 m.

Within the contour-line buffers on the ice caps, the average differences are -3.9 ± 10-m rms between GLAS and ASTER elevations (-3.8 m with GLAS saturation correction applied; -1.5 m/year), -20.4 ± 18-m rms between GLAS and 1970/1971 contour-line elevations (-20.3 m with saturation correction applied; -0.62 m/year), and -16.5 ± 21-m rms between ASTER and the 1970/1971 contour elevations (-0.53 m/year) (method 6); Table II, cf. Fig. 7). These numbers coincide well with the difference calculations for the entire nonbuffered data set within the ice-cap boundaries and suggest, therefore, that the GLAS tracks and footprints cover a representative subset of the ice caps.

Calculating the average elevation difference between contour-line buffers and GLAS elevations at each 50-m elevation level and multiplying these numbers with the total glacier area of this elevation interval (hypsography in Fig. 8) gives an average elevation change of -19.7 m for both ice caps together [-0.58 m/year; method 7)].

Plotting the elevation changes between 1970/1971 and the ICESat acquisitions against elevation (method 8); Fig. 8) shows that the overall relation between elevation change versus elevation is quite similar to the corresponding ASTER-derived relation, although the ICESat tracks overlap only with a small fraction of the glacier areas. Integrating the ICESat-derived relation over the entire ice-cap areas gives an average elevation loss of -20.4 m (-0.62 m/year).

C. Glacier Volume Change

The strongest elevation loss for both ice caps can be found at around 100-m above sea level (a.s.l.), i.e., at the termini of the outlet glaciers (Figs. 6–8). The decrease of elevation loss toward altitudes below 100-m a.s.l. is due to the debris cover at the glacier snouts that reduces the melt of the underlying ice and due to the fact that the glaciers retreated between 1970 and 2002 or 2006, respectively, which stabilized the elevation at places where the ice disappeared before 2002 or 2006. Toward the highest parts of the ice caps, thickness losses tend to small values or even zero (Figs. 7 and 8). The raw and interpolated elevation differences (Figs. 5–7) show even a zone of slight thickness increase in the top region, however, within the significance level of the method.

The ice-thickness change over time at an individual point is the result of the mass balance at this point and the divergence of flux at this point. The latter is a function of, among others, ice dynamics and glacier bed and glacier surface topographies. When averaging over an entire glacier, the mean divergence of flux becomes zero, which allows one in computing mean glacier mass balance from thickness changes when these cover the entire glacier—the target of this paper. The general pattern of elevation changes found here with largest thickness losses at the lower elevations is very common for retreating glaciers and most likely reflects the ice-dynamical and geometric adjustments of the glaciers to a negative mass balance [24].

Averaging the results from methods 1)–4) gives an overall thickness loss of -17.5 ± 0.5-m rms between 1970/1971 and 2002 (-0.55 m/year) (Table I). Assuming an ice density of 0.9 gives -15.8-m water equivalent (w.e.) (-0.50 m $\cdot$ w.e./year). The latter corresponds to a volume loss of 6 km$^3 \cdot$ w.e. over 30 years. The numbers for the total volume change of Digerfonna and Kvalpyntfonna between 1970/1971 and 2002 correspond very well with geodetic and glaciological mass-balance measurements on Svalbard, mainly performed in western Spitsbergen [19], [25]. Current glacial rebound rates on Svalbard are on the order of millimeters per year [26], [27] and are thus several orders of magnitude smaller than the elevation changes found here.

Using the ICESat-derived instead of the ASTER-derived elevation data reveals an overall elevation change between

1970/1971 and 2006 of −21.8 m (−21.7 m with saturation correction applied; −0.61 m/year, −0.54 m · w.e./year). The elevation differences between the 2002 ASTER DTM and the 2003–2006 GLAS data should be interpreted with caution, because we have no snow-depth data or sufficient ICESat repeat-track overlaps or crossovers to estimate snow-depth changes reliably. If, however, we correct the elevation differences between ASTER and GLAS over the ice caps using the corresponding average offsets from outside the ice caps, we obtain an elevation change of −0.8 m/year (−0.7 m · w.e./year) between 2002 and 2006. Again, this value coincides well with mass-balance measurements from western Spitsbergen, which also indicate an increasingly negative glacier mass trend in recent years [25], [28].

IV. Discussion and Conclusion

Our test study shows that even medium-resolution optical satellite stereo sensors such as ASTER can be used to derive glacier elevation changes over several decades, when compared to preexisting elevation data. In most cases, the latter base data will have been directly derived from stereo airphotos using photogrammetric techniques [8] or be digitized from existing topographic maps.

Table II summarizes the comparisons between the different elevation data sets. The rms values in Table II are the combined accuracy from both data sets compared and temporal variations between them (RSS) and can thus be interpreted as the maximum uncertainty of the individual data sets. By comparing the ASTER DTM to ICESat GLAS elevation data over the ice caps, we estimate therefore a vertical rms error of individual ASTER DTM points or ICESat-derived elevations of certainly better than ±12 m over the glacier areas. This value is better than our *a priori* estimate of ±15-m rms for ASTER (= ASTER VNIR pixel size) and suggests that the topographic and radiometric conditions of the glaciers and images studied are very favorable for photogrammetric DTM generation [8], [12]. Outside the glacier boundaries, we obtain an rms deviation of better than ±24 m between the ASTER DTM and the ICESat data. This decreased accuracy is expected for the mountainous topography on Edgeøya, which reduces the accuracy of both the GLAS and ASTER elevations. In addition, the low radiometric contrast of the largely featureless plateau surfaces reduces the ASTER parallax matching accuracy (Fig. 3).

The comparison between the ICESat-derived elevations and the 1970/1971 contour lines suggests that the accuracies of the contour-line and ICESat elevations are certainly better than ±12 m. With the data sets available to us, we cannot reliably estimate the accuracy of the ICESat-derived elevations for our test site. From the topographic conditions, it is, however, clear that the accuracy will be much less than the few centimeters achievable for ice sheets or lake ice [14], [23] but, rather, on the order of several decimeters to meters. The comparison between the GLA06 and GLA14 products presented in Section II-C can be taken as a rough hint to that order of magnitude.

The good agreement between the volume changes derived from ASTER and the ones derived from ICESat GLAS suggests that even ICESat tracks with sparse overlap over the elevation zones of a glacier may be useful to estimate glacier volume changes if ICESat tracks cover a representative portion of the glaciers, such as all elevation zones, and if the ice thickness changes observed show no large spatial variability. The availability of ICESat data over large scales makes it, thus, a promising tool for investigating regional-scale volume changes of glaciers.

Due to the rms error of individual ASTER DTM points and the contour lines, individual elevation differences between both data sets are only significant at low altitudes of the ice caps (see also Fig. 7). Similarly, the elevation differences at individual points between ICESat-derived elevations and the contour lines are hardly significant at the higher altitudes but clearly at lower altitudes.

However, the standard error of the mean elevation difference over the ice caps is significantly lower than the rms of an individual elevation difference. The standard error of the mean would be the rms error divided by the root of the number of measurements in case of a constant elevation change on the ice caps and a randomly (Gaussian) distributed vertical error of the elevation differences (cf. [4]). This hypothesis is not valid for the following several reasons: 1) the elevation change is spatially variable so that its standard error becomes the RSS of this spatial variance and the standard error of the measurements; 2) while the accuracy of the ICESat-derived elevations may approximate Gaussian distribution, this is presumably less the case for the contour lines and much less for the ASTER-derived elevations. Neighboring ASTER elevations are correlated due to the photogrammetric image-pyramid approach and the overlap of the moving parallax matching window.

Within the contour-line buffers, approximately 180 GLAS footprints were used and ca. 400 for the entire ice caps. Dividing the rms values given in Table II by the root of these numbers indicates a standard error of at least ±1 m. Assuming, arbitrarily, that ASTER-derived elevations that are 1 km apart are not correlated gives a number of ca. 350 "independent" ASTER elevations on the ice caps. Dividing the rms values in Table II by the root of this number and keeping in mind that the rms values for the glaciated area are, to a large extent, also due to the spatial variability of the elevation changes observed (RSS) indicates that the standard error of the mean elevation change is certainly better than ±1 m.

The difference between the calculation methods 1)–4) based on the ASTER DTM offers a further accuracy check and provides an rms error of the mean elevation change of ±0.5 m. The difference between these ASTER-based approaches to the ICESat-based approach is ±1.3 m. All the estimates, together from this and the latter paragraph, lead us to expect that the glacier volume changes computed have a standard error on the order of roughly 5%.

In our test study, the almost complete disappearance of the winter snow over the entire ice caps in summer 2002 led to good radiometric contrast over wide areas of the glaciers. This allowed for reliable photogrammetric generation of an ASTER DTM over the entire glaciated area and, thus, for determining the total volume change of the ice caps. Such near-complete loss of snow cover over entire glaciers can be more frequently observed in recent years for low-elevation glaciers as a result of increasingly negative glacier mass balances worldwide. Satellite optical stereo, often hampered by the lack of radiometric contrast over snow and firn, may thus become more and more applicable for determining changes in thickness and volume of glaciers and ice caps. This situation improves when considering high-resolution satellite optical stereo sensors such as SPOT5 HRS or ALOS PRISM. Where available, the DTM from the SRTM in 2000 can be used as baseline data to compare with DTMs from satellite optical stereo [5], [11] and GLAS elevation data [3], [15].

Ultimately, we favor a combination of satellite stereo, laser altimetry, SAR interferometry, and preexisting elevation data for global-scale monitoring of glacier volume changes. Combination with radar altimetry may become potentially useful for typical glacier topography with the advent of the CRYOSAT-2 interferometric radar altimeter SIRAL.

ACKNOWLEDGMENT

The author would like to thank J. Kohler and an anonymous referee for their very thorough and constructive comments. The ASTER scene applied in this paper was provided within the framework of the Global Land Ice Measurements from Space project (GLIMS) through the EROS data centre and is courtesy of NASA/GSFC/METI/ERSDAC/JAROS and the US/Japan ASTER science team. The ICESat GLAS data were obtained from the NSIDC, Boulder.

REFERENCES

[1] E. Rignot, A. Rivera, and G. Casassa, "Contribution of the Patagonia Icefields of South America to sea level rise," *Science*, vol. 302, no. 5644, pp. 434–437, Oct. 2003.

[2] E. Berthier, Y. Arnaud, C. Vincent, and F. Remy, "Biases of SRTM in high-mountain areas: Implications for the monitoring of glacier volume changes," *Geophys. Res. Lett.*, vol. 33, no. 8, L08 502, Apr. 2006.

[3] J. Sauber, B. Molnia, C. Carabajal, S. Luthcke, and R. Muskett, "Ice elevations and surface change on the Malaspina Glacier, Alaska," *Geophys. Res. Lett.*, vol. 32, no. 23, p. L23 S01, Oct. 2005.

[4] E. Berthier, Y. Arnaud, D. Baratoux, C. Vincent, and F. Remy, "Recent rapid thinning of the 'Mer de Glace' glacier derived from satellite optical images,"*Geophys. Res. Lett.*, vol. 31, no. 17, L17 401, Sep. 2004.

[5] E. Berthier, Y. Arnaud, R. Kumar, S. Ahmad, P. Wagnon, and P. Chevallier, "Remote sensing estimates of glacier mass balances in the Himachal Pradesh (Western Himalaya, India)," *Remote Sens. Environ.*, vol. 108, no. 3, pp. 327–338, Jun. 2007.

[6] E. Berthier and T. Toutin, "SPOT5-HRS digital elevation models and the monitoring of glacier elevation changes in north–west Canada and south–east Alaska," *Remote Sens. Environ.*, vol. 112, no. 5, pp. 2443–2454, May 2008.

[7] A. Rivera, G. Casassa, J. Bamber, and A. Kääb, "Ice elevation changes of Glaciar Chico in the Southern Patagonia Icefield, using ASTER DEMs, aerial photographs and GPS data," *J. Glaciol.*, vol. 51, no. 172, pp. 105–112, Jan. 2005.

[8] A. Kääb, *Remote Sensing of Mountain Glaciers and Permafrost Creep*, vol. 48. Zurich, Switzerland: Univ. Zurich, 2005.

[9] F. Vignon, Y. Arnaud, and G. Kaser, "Quantification of glacier volume change using topographic and ASTER DEMs," in *Proc. IGARSS*, 2003, vol. 4, pp. 2605–2607.

[10] S. J. S. Khalsa, M. B. Dyurgerov, T. Khromova, B. H. Raup, and R. G. Barry, "Space-based mapping of glacier changes using ASTER and GIS tools," *IEEE Trans. Geosci. Remote Sens.*, vol. 42, no. 10, pp. 2177–2183, Oct. 2004.

[11] A. E. Racoviteanu, W. F. Manley, Y. Arnaud, and M. W. Williams, "Evaluating digital elevation models for glaciologic applications: An example from Nevado Coropuna, Peruvian Andes," *Glob. Planet. Change*, vol. 59, no. 1-4, pp. 110–125, Oct. 2007.

[12] T. Toutin, "Three-dimensional topographic mapping with ASTER stereo data in rugged topography," *IEEE Trans. Geosci. Remote Sens.*, vol. 40, no. 10, pp. 2241–2247, Oct. 2002.

[13] A. Kääb, "Monitoring high-mountain terrain deformation from air- and spaceborne optical data: Examples using digital aerial imagery and ASTER data," *ISPRS J. Photogramm. Remote Sens.*, vol. 57, no. 1/2, pp. 39–52, Nov. 2002.

[14] H. J. Zwally, B. Schutz, W. Abdalati, J. Abshire, C. Bentley, A. Brenner, J. Bufton, J. Dezio, D. Hancock, D. Harding, T. Herring, B. Minster, K. Quinn, S. Palm, J. Spinhirne, and R. Thomas, "ICESat's laser measurements of polar ice, atmosphere, ocean, and land," *J. Geodyn.*, vol. 34, no. 3/4, pp. 405–445, Oct./Nov. 2002.

[15] A. B. Surazakov and V. B. Aizen, "Estimating volume change of mountain glaciers using SRTM and map-based topographic data," *IEEE Trans. Geosci. Remote Sens.*, vol. 44, no. 10, pp. 2991–2995, Oct. 2006.

[16] E. Rignot, G. Casassa, S. Gogineni, P. Kanagaratnam, W. Krabill, H. Pritchard, A. Rivera, R. Thomas, J. Turner, and D. Vaughan, "Recent ice loss from the Fleming and other glaciers, Wordie Bay, West Antarctic Peninsula," *Geophys. Res. Lett.*, vol. 32, no. 7, L07 502, Apr. 2005.

[17] T. Schenk, B. Csatho, C. J. van der Veen, H. Brecher, Y. Ahn, and T. Yoon, "Registering imagery to ICESat data for measuring elevation changes on Byrd Glacier, Antarctica," *Geophys. Res. Lett.*, vol. 32, no. 23, L23 S05, Dec. 2005.

[18] J. A. Dowdeswell and J. L. Bamber, "On the glaciology of Edgeøya and Barentsøya, Svalbard," *Polar Res.*, vol. 14, no. 2, pp. 105–122, 1995.

[19] J. O. Hagen, J. Kohler, K. Melvold, and J. G. Winther, "Glaciers in Svalbard: Mass balance, runoff and freshwater flux," *Polar Res.*, vol. 22, no. 2, pp. 145–159, 2003.

[20] H. J. Zwally, R. Schutz, C. Bentley, J. Bufton, T. Herring, J. Minster, J. Spinhirne, and R. Thomas, *GLAS/ICESat L2 Global Land Surface Altimetry Data V028*. Boulder, CO: Nat. Snow Ice Data Center. Digital Media, 2007.

[21] A. C. Brenner, C. R. Bentley, B. M. Csatho, D. J. Harding, M. A. Hofton, J. Minster, L. Roberts, J. L. Saba, R. Schutz, R. H. Thomas, D. Yi, and H. J. Zwally, *Derivation of Range and Range Distributions From Laser Pulse Waveform Analysis for Surface Elevations, Roughness, Slope, and Vegetation Heights.* Algorithm Theoretical Basis Document. Greenbelt, MD: Goddard Space Flight Center, 2003. Version 3.0.

[22] F. Paul, A. Kääb, M. Maisch, T. Kellenberger, and W. Haeberli, "Rapid disintegration of Alpine glaciers observed with satellite data,"*Geophys. Res. Lett.*, vol. 31, no. 21, L21 402, Nov. 2004.

[23] D. K. Atwood, R. M. Guritz, R. R. Muskett, C. S. Lingle, J. M. Sauber, and J. T. Freymuler, "DEM control in Arctic Alaska with ICESat laser altimetry," *IEEE Trans. Geosci. Remote Sens.*, vol. 45, no. 11, pp. 3710–3720, Nov. 2007.

[24] M. P. Schwitter and C. F. Raymond, "Changes in the longitudinal profiles of glaciers during advance and retreat," *J. Glaciol.*, vol. 39, no. 133, pp. 582–590, 1993.

[25] J. Kohler, T. D. James, T. Murray, C. Nuth, O. Brandt, N. E. Barrand, H. F. Aas, and A. Luckman, "Acceleration in thinning rate on western Svalbard glaciers,"*Geophys. Res. Lett.*, vol. 34, no. 18, L18 502, Sep. 2007.

[26] S. Bondevik, J. Mangerud, L. Ronnert, and O. Salvigsen, "Postglacial sea-level history of Edgeoya and Barentsoya, eastern Svalbard," *Polar Res.*, vol. 14, no. 2, pp. 153–180, 1995.

[27] T. Sato, J. Okuno, J. Hinderer, D. S. MacMillan, H. P. Plag, O. Francis, R. Falk, and Y. Fukuda, "A geophysical interpretation of the secular displacement and gravity rates observed at Ny–Alesund, Svalbard in the Arctic—effects of post-glacial rebound and present-day ice melting," *Geophys. J. Int.*, vol. 165, no. 3, pp. 729–743, Jun. 2006.

[28] C. Nuth, "Geodetic mass balance of Svalbard glaciers : 1936–2004," M.S. thesis, Univ. Oslo, Oslo, Norway, 2006.

Andreas Kääb (M'07) received the Diploma degree in geomatics engineering from the Technical University of Munich, Munich, Germany, in 1990, the Ph.D. degree in earth sciences from the Versuchsanstalt für Wasserbau, Hydrologie und Glaziologie, Eidgenoessische Technische Hochschule (ETH) Zürich, Zürich, Switzerland, in 1996, and the Habilitation degree in physical geography from the University of Zürich, Zürich, in 2004.

He is currently a Professor in remote sensing with the Department of Geosciences, University of Oslo, Oslo, Norway, where he is focusing, among others, on methods for the observation of climate change impacts on glaciers, permafrost, and the hazards related to these. He has published a book on remote sensing of mountain glaciers and permafrost creep.

Dr. Kääb is, among others, a member of the American Geophysical Union, European Geosciences Union, and International Glaciological Society.